INTERNATIONAL JOURNAL FOR NUMERICAL METHODS IN ENGINEERING, VOL. 40, 1335–1354 (1997)

FINITE ELEMENT STRESS EXTRACTION BY THE COMPLEMENTARY ENERGY PRINCIPLE

ZOHAR YOSIBASH

Pearlstone Center for Aeronautical Engineering Studies, Department of Mechanical Engineering, Ben-Gurion University of the Negev, Beer-Sheva, Israel

SUMMARY

This paper presents a new method for accurate pointwise stress extraction from finite element solutions, applied to two-dimensional linear elastostatic problems having bounded value stresses. The method, denoted by *SEC* (Stress Extraction by Complementary principle), is based on the complementary energy principle applied over a local domain in the post-processing phase. Detailed formulation of the SEC method is provided, and numerical experiments with the *h*- and *p*-versions of the finite element method are presented for a family of exact solutions characterized by varying degree of smoothness. It is shown that on the boundaries of the domain, as well as in the interior, accurate pointwise stresses are obtained, and the relative error in the pointwise stresses converges with a rate which is as fast as the relative error measured in energy norm or faster. Importantly, the SEC method in conjunction with the *p*-version of the finite element method is virtually independent of the Poisson's ratio,[1] and is equally applicable to nearly incompressible materials.

KEY WORDS: finite element methods; complementary energy; *p*-version; stress extraction

1. INTRODUCTION

Displacement-based Finite Element (FE) methods, formulated based on the principle of minimum potential energy, maintain only C^0 continuity over the problem domain, and the convergence of the numerical approximation to the exact value is usually measured in the energy norm, which is a global measure. Analysts, however, are interested in pointwise stresses rather than energy, and the problem of stress extraction from FE solutions has been the subject of many investigations. Typically, the pointwise stresses are obtained 'directly' from the FE solution, that is, by differentiating the displacement function to obtain the strain components, then using the strain–stress law for computing the stresses (see detailed description in Section 11.4.1 of Reference 2). The pointwise stresses computed by the direct method do not (in general) converge monotonically (even though the error in energy norm does), and their rate of convergence usually depends on the smoothness of the exact solution. Only when the exact solution is relatively smooth, one observes that the stresses extracted by the direct method converge in a satisfactory manner, and their rates of convergence are similar to that of the energy norm when the latter is sufficiently small. This behaviour was demonstrated in Reference 3. As the exact solution becomes progressively less smooth, the performance of the direct method deteriorates, and indirect extraction methods should be sought.

Indirect computation of stresses have been shown to be superior to direct methods (see for example References 4–9 and the references therein). The methods presented in References 4–7 are based on specially constructed extraction functions, so that some measure of artificial intelligence should be applied in a general purpose computer programs in the sense that the proper extraction

CCC 0029–5981/97/071335–20$17.50

Received 17 December 1995
Revised 31 July 1996

functions must be selected automatically, depending on the problem parameters and the *location* of output information required (this holds true for the SEC method, but in a smaller extent). Computer implementation of these indirect methods is difficult, because different procedures are required at and near boundaries as opposed to the interior. The author does not know of any practical implementation of indirect extraction techniques for the pointwise stresses, even though the methods have been known for more than 10 years. The patch recovery method in Reference 8 requires the existence of superconvergent points and does not perform satisfactorily in the neighbourhood of steep stress gradients. In Reference 9 a technique based on local interpolation of nodal displacements using the moving least-squares method is presented which demonstrates good results for the extracted stresses for many of the cases studied. For nearly incompressible materials, the performance of the mentioned indirect methods is expected to deteriorate considerably, except for the methods presented in References 4 and 5.

The SEC method presented in this paper in the framework of two-dimensional elastostatics is equally suited for nearly incompressible materials when applied in conjunction with the *p*-version of the FEM,[1] is fully general, and may be implemented in any finite element code. It is a post-processing technique, namely, after the displacement-based FE analysis is completed, the displacements approximation is used for further computations to obtain results of higher accuracy. The formulation of the method, based on the principle of minimum complementary energy, is presented for stress computation at interior and boundary points. Pointwise stresses extracted by SEC are documented for a family of problems for which the exact solution is known and the smoothness of the solution is varied. Mathematical analysis on convergence rates of the SEC is not discussed.

An outline of the paper is as follows. Notations and detailed formulation of the suggested extraction method is followed. In Section 3 we describe the family of problems for which the exact solution is known. These problems are solved by the *p*-version of the finite element method, and the stresses are extracted by the direct and by the SEC methods and compared to the exact values. The performance of the SEC in conjunction with the *h*-version of the FEM is documented in Section 4. We finally present a summary and conclusions in Section 5.

2. SEC METHOD

2.1. Notations and preliminaries

The problem of interest is the linear plane elasticity in an isotropic domain without body forces or thermal loading. Let Ω be a two-dimensional linear elastic domain with a boundary denoted by $\partial\Omega$ and let $\Omega_R \subset \Omega$. The displacements vector expressed in a Cartesian co-ordinate system is denoted by $\mathbf{u} \stackrel{\text{def}}{=} (u_1, u_2)^{\mathrm{T}}$ and the linear strain tensor by

$$\varepsilon_{ij}(\mathbf{u}) = \frac{1}{2}\left(\frac{\partial u_i}{\partial x_j} + \frac{\partial u_j}{\partial x_i}\right)$$

Throughout the paper the stress tensor in two dimensions will be denoted either by its tensor or vector form,

$$\underset{\approx}{\boldsymbol{\sigma}} \stackrel{\text{def}}{=} \begin{bmatrix} \sigma_{11} & \sigma_{12} \\ \sigma_{12} & \sigma_{22} \end{bmatrix} \quad \text{or} \quad \boldsymbol{\sigma} \stackrel{\text{def}}{=} \begin{Bmatrix} \sigma_{11} \\ \sigma_{22} \\ \sigma_{12} \end{Bmatrix}$$

The constitutive law (Hooke's law) for an isotropic two-dimensional elastic domain is given by

$$[C]\boldsymbol{\sigma} = \boldsymbol{\epsilon} \stackrel{\text{def}}{=} (\varepsilon_{11}, \varepsilon_{22}, \varepsilon_{12})^{\mathrm{T}} \tag{1}$$

where

$$[C] = \frac{1+v}{2E}\begin{bmatrix} c+1 & c-1 & 0 \\ c-1 & c+1 & 0 \\ 0 & 0 & 2 \end{bmatrix}$$

$c = 1 - 2v$ for plane-strain situation, $c = (1-v)/(1+v)$ for plane-stress situation and E and v are the Young's modulus and the Poisson's ratio, respectively.

We denote the inner product of the $\mathbf{L}^2(\Omega)$ space for a vector function or a tensor by

$$(\boldsymbol{\sigma}, \boldsymbol{\tau})_{\mathbf{L}^2,\Omega} \stackrel{\text{def}}{=} \iint_\Omega \boldsymbol{\sigma}^{\mathrm{T}}\boldsymbol{\tau}\, \mathrm{d}\Omega$$

$$\left(\underset{\approx}{\boldsymbol{\sigma}}, \underset{\approx}{\boldsymbol{\tau}}\right)_{\mathbf{L}^2,\Omega} \equiv \iint_\Omega \underset{\approx}{\boldsymbol{\sigma}} : \underset{\approx}{\boldsymbol{\tau}}\, \mathrm{d}\Omega \stackrel{\text{def}}{=} \iint_\Omega \sum_i \sum_j \sigma_{ij}\tau_{ij}\, \mathrm{d}\Omega \tag{2}$$

with the corresponding norm $\| \bullet \|_{\mathbf{L}^2,\Omega} \stackrel{\text{def}}{=} \sqrt{(\bullet,\bullet)_{\mathbf{L}^2,\Omega}}$. Notice that

$$\sqrt{2}\|\boldsymbol{\sigma}\|_{\mathbf{L}^2,\Omega} \geqslant \| \underset{\approx}{\boldsymbol{\sigma}} \|_{\mathbf{L}^2,\Omega} \geqslant \|\boldsymbol{\sigma}\|_{\mathbf{L}^2,\Omega}.$$

The div and grad operators on vectors and **div**, **grad** operators on tensors are defined according to Chapter 9 of Reference 10. We denote the Sobolev space for a vector function excluding rigid body motions by $\mathbf{H}^1(\Omega)$:

$$\mathbf{H}^1(\Omega) = \{\mathbf{u} \mid \sqrt{\|\mathrm{grad}\,\mathbf{u}\|^2_{\mathbf{L}^2,\Omega} + \|\mathbf{u}\|^2_{\mathbf{L}^2,\Omega}} < \infty\} \;\setminus\; \{\text{Rigid body motions}\}$$

with $\| \bullet \|_{1,\Omega}$ denoting the corresponding norm. Let $\boldsymbol{\Sigma}(\Omega_R)$ be the statically admissible space defined by

$$\boldsymbol{\Sigma}(\Omega_R) = \{\underset{\approx}{\boldsymbol{\sigma}} \mid \| \underset{\approx}{\boldsymbol{\sigma}} \|_{\mathbf{L}^2,\Omega_R} < \infty;\ \mathbf{div}\ \underset{\approx}{\boldsymbol{\sigma}} = \mathbf{0} \text{ in } \Omega_R\}$$

and let $\boldsymbol{\Sigma}^N(\Omega_R)$ be a subspace of $\boldsymbol{\Sigma}(\Omega_R)$ with $\dim \boldsymbol{\Sigma}^N(\Omega_R) = N < \infty$.

We introduce the two bilinear forms associated with the primal and dual weak formulations:

$$\mathscr{B}(\mathbf{u},\mathbf{v}) = \iint_\Omega [2\mu\, \underset{\approx}{\boldsymbol{\epsilon}}(\mathbf{u}) : \underset{\approx}{\boldsymbol{\epsilon}}(\mathbf{v}) + \bar{\lambda}\, \mathrm{div}\,\mathbf{u} \cdot \mathrm{div}\,\mathbf{v}]\mathrm{d}\Omega \tag{3}$$

$$\mathscr{B}_{\mathrm{c}}(\boldsymbol{\sigma},\boldsymbol{\sigma}_{\mathrm{o}}) = \iint_{\Omega_R} \boldsymbol{\sigma}^{\mathrm{T}}[C]\boldsymbol{\sigma}_{\mathrm{o}}\, \mathrm{d}\Omega. \tag{4}$$

and their corresponding norms, defined as follows:

$$\|\mathbf{u}\|_{\mathscr{B},\Omega} \stackrel{\text{def}}{=} \sqrt{\frac{1}{2}\mathscr{B}(\mathbf{u},\mathbf{u})} = \frac{1}{\sqrt{2}}(2\mu\| \underset{\approx}{\boldsymbol{\epsilon}}(\mathbf{u})\|^2_{0,\Omega} + \bar{\lambda}\|\mathrm{div}\,\mathbf{u}\|^2_{0,\Omega})^{1/2}$$

called the '*energy norm*', and

$$\|\boldsymbol{\sigma}\|_{\mathscr{B}_c,\Omega_R} \stackrel{\text{def}}{=} \sqrt{\frac{1}{2}\mathscr{B}_c(\boldsymbol{\sigma},\boldsymbol{\sigma})}$$

$$\bar{\lambda} = \begin{cases} \lambda & \text{for plane-strain} \\ 2\lambda\mu/(\lambda+2\mu) & \text{for plane-stress} \end{cases}$$

where μ, λ are the Lamé constants, expressed in terms of E and v as follows:

$$\mu = \frac{E}{2(1+v)}, \quad \lambda = \frac{Ev}{(1+v)(1-2v)}$$

The linear continuous forms associated with the primal and dual weak formulations are defined as

$$\mathscr{F}(\mathbf{v}) = \int_{\Gamma_T} \mathbf{v}^T \cdot \mathbf{t}\, ds \tag{5}$$

$$\mathscr{F}_c(\boldsymbol{\sigma}_o) = \int_{(\Gamma_R)_u} \hat{\mathbf{u}}^T \cdot ([n]\boldsymbol{\sigma}_o)\, ds \tag{6}$$

where Γ_T denotes the part of the boundary $\partial\Omega$ where traction boundary conditions $\mathbf{t}$ are prescribed, $(\Gamma_R)_u$ denotes the part of the boundary $\partial\Omega_R$ where displacement boundary conditions $\hat{\mathbf{u}}$ are prescribed,

$$[n] = \begin{bmatrix} n_1 & 0 & n_2 \\ 0 & n_1 & n_2 \end{bmatrix}$$

and $\mathbf{n} \stackrel{\text{def}}{=} (n_1, n_2)$ is the outward normal vector to the boundary.

The primal weak formulation (also known as the displacement weak formulation) equivalent to the elasticity Lamé–Navier equations is cast in the form:

$$\text{Seek } \mathbf{u} \in \mathbf{H}^1(\Omega) \text{ such that}$$

$$\mathscr{B}(\mathbf{u},\mathbf{v}) = \mathscr{F}(\mathbf{v}) \quad \forall \mathbf{v} \in \mathbf{H}^1(\Omega) \tag{7}$$

If also homogeneous Dirichlet boundary conditions are specified on $\Gamma_D \subset \partial\Omega$ (a part of the boundary), $\mathbf{u}$ and $\mathbf{v}$ in (7) are required to lie in the space $\overset{o}{\mathbf{H}}{}^1(\Omega)$ defined by

$$\overset{o}{\mathbf{H}}{}^1(\Omega) \left\{ \mathbf{u} \;\middle|\; \mathbf{u} \in \mathbf{H}^1(\Omega),\ \mathbf{u} = \mathbf{0} \text{ on } \Gamma_D \right\}.$$

The dual (complementary) weak formulation of the elasticity problem over the sub-domain Ω_R is

$$\text{Seek } \boldsymbol{\sigma} \in \Sigma(\Omega_R) \text{ such that}$$
$$\mathscr{B}_c(\boldsymbol{\sigma},\boldsymbol{\sigma}_o) = \mathscr{F}_c(\boldsymbol{\sigma}_o) \quad \forall \boldsymbol{\sigma}_o \in \Sigma(\Omega_R) \tag{8}$$

2.2. The SEC method

The complementary weak form (8) is used for pointwise stress extraction. The procedure is a post-solution operation performed after the elastostatic problem over Ω is solved by the FEM based on the displacement formulation (7) and having obtained $\mathbf{u}^{FE}$.

Assume that the stresses at a specific point are of interest. A subdomain around that point is selected, depending on whether the point O is an internal point, the point Q is on a smooth

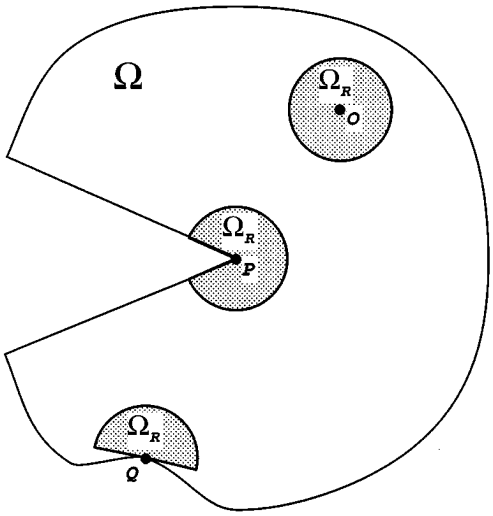

Figure 1. Typical points of interest in a domain

boundary or the point P is a point where the stresses are singular, see Figure 1. Define S_R as the interior points of a circle of radius R centred on the point of interest. For points O and P, Ω_R is defined by $\Omega \cap S_R$. For point Q we define Ω_R as the half circle $\Omega \cap S_R \cap$ the half plane defined by the straight tangent line to the boundary at the point Q. In the following, only points O and Q, where the stresses are regular, are treated. A detailed treatment for point P, where the stresses are singular, can be found in References 11 and 12.

We discretize the complementary weak form (8) over Ω_R by choosing a sequence of finite-dimensional subspaces $\Sigma^N(\Omega_R) \subset \Sigma(\Omega_R)$ (N denoting the dimension, and as will be shown in the following, it depends on Airy's stress function polynomial order). Any $\boldsymbol{\sigma}$ which belongs to $\Sigma^N(\Omega_R)$ can be written in the form

$$\boldsymbol{\sigma}(r, \theta) = \sum_{i=1}^{N} a_i \mathbf{f}_i(r, \theta) \tag{9}$$

where r, θ are the co-ordinates of a cylindrical co-ordinate system located at the point of interest and $\mathbf{f}_i = (f_{11},\ f_{22},\ f_{12})_i^{\mathrm{T}}$ are smooth vector functions which have to lay in the statically admissible space $\Sigma(\Omega_R)$. On the boundary $\partial\Omega_R$, we impose displacement boundary conditions obtained by the FE analysis, $\mathbf{u}^{\mathrm{FE}}$. The functions $\mathbf{f}_i \in \Sigma(\Omega_R)$ are derived from an Airy stress function $\Phi_i(\xi, \eta)$. Many statically admissible spaces can be constructed, and we concentrate our discussion in the next subsection on two possibilities.

On $\partial\Omega_R$ the finite element solution obtained by the displacement formulation ($\mathbf{u}^{\mathrm{FE}}$) is prescribed, thus the discretized complementary weak form (8) is equivalent to solving

$$[B_{\mathrm{c}}]\mathbf{a} = \mathbf{F}_{\mathrm{c}} \tag{10}$$

where $\mathbf{a} = (a_1,\ a_2, \ldots,\ a_N)^{\mathrm{T}}$, $[B_{\mathrm{c}}]$ is an $N \times N$ matrix and $\mathbf{F}_{\mathrm{c}}$ is a vector defined by

$$\begin{aligned}(B_{\mathrm{c}})_{ij} = \int_0^R \int_{\theta_1}^{\theta_2} \{ & C_1(f_{11})_i(f_{11})_j + C_3(f_{22})_i(f_{22})_j + C_6(f_{12})_i(f_{12})_j \\ & + C_2(f_{11})_i(f_{22})_j + C_4(f_{11})_i(f_{12})_j + C_5(f_{22})_i(f_{12})_j \\ & + C_2(f_{22})_i(f_{11})_j + C_4(f_{12})_i(f_{11})_j + C_5(f_{12})_i(f_{22})_j \}\, r\, \mathrm{d}r\, \mathrm{d}\theta \quad i, j = 1, 2, \ldots, N\end{aligned} \tag{11}$$

$$(F_c)_j = \int_{\partial\Omega_R} \left(\mathbf{u}^{FE}\right)^T \begin{Bmatrix} \cos\theta (f_{11})_j + \sin\theta (f_{12})_j \\ \sin\theta (f_{22})_j + \cos\theta (f_{12})_j \end{Bmatrix} ds, \quad j = 1, 2, \ldots, N \tag{12}$$

where $C_1 = C_{11}, C_2 = C_{12}, C_3 = C_{22}, C_4 = C_{13}, C_5 = C_{23}$, and $C_6 = C_{33}$. For points within the domain (as point O) $\theta_1 = 0$, $\theta_2 = 2\pi$, whereas for points on the boundary (as point Q) $\theta_1 = \beta$ and $\theta_2 = \beta + \pi$, β being the angle between the inward normal vector to the boundary at Q and the x_1-axis. The entries of the matrix $[B_c]$ can be pre-computed analytically because the vectors $\mathbf{f}_i$ are simple polynomials in r and sin θ or cos θ, and the material properties within Ω_R are assumed to be fixed. The entries of the vector $\mathbf{F}_c$ are computed by Gaussian quadrature of order 14.

Remark 1. The SEC method does not distinguish between cases when stresses are sought on the boundaries or in the interior of the domain. When boundary stresses are sought, the same technique applies whether tractions or displacements are specified as boundary conditions.

Remark 2. Unlike FEM based entirely on complementary energy principle, requiring C^1 continuous elements, the SEC method does not require any such constraints.

Remark 3. It should be emphasized that the SEC method is a localized operation applied over a standard circular type domain.

Solving (10), one obtains an approximation for $\mathbf{a}$, and the SEC stresses at the point of interest are given by

$$\boldsymbol{\sigma} = \sum_{i=1}^{N} a_i \mathbf{f}_i(0,0) \tag{13}$$

2.3. Constructing the statically admissible space

2.3.1. The equilibrated space. Any vector $\mathbf{f}_i$ which is derived from an Airy polynomial function $\Phi_i(\xi,\eta)$ by the relation

$$\mathbf{f}_i = \begin{cases} \dfrac{\partial^2 \Phi_i(\xi,\eta)}{\partial \eta^2} \\ \dfrac{\partial^2 \Phi_i(\xi,\eta)}{\partial \xi^2} \\ -\dfrac{\partial^2 \Phi_i(\xi,\eta)}{\partial \xi \partial \eta} \end{cases} \tag{14}$$

satisfies identically the equilibrium equation, therefore lies in the statically admissible space. The polynomials $\Phi_i(\xi,\eta)$ are constructed as a product of two Legendre polynomials:

$$\Phi_i(\xi,\eta) = P_j(\xi) P_k(\eta), \quad j, k = 0, 1, \ldots, 9 \rightarrow i = 0, 1, \ldots, 100$$

where P_j is the Legendre polynomials of degree j, $\xi = r\cos\theta$ and $\eta = r\sin\theta$. For any combination of j and k, the vector $\mathbf{f}_i$ is computed:

$$\mathbf{f}_i = \begin{cases} P_j(\xi) \frac{\partial^2 P_k(\eta)}{\partial \eta^2} \\ P_k(\eta) \frac{\partial^2 P_j(\xi)}{\partial \xi^2} \qquad j, k = 0, 1, \ldots, 9 \\ -\frac{\partial^2 (P_j(\xi) P_k(\eta))}{\partial \xi \partial \eta} \end{cases}$$

Choosing Legendre polynomials up to degree 8 ($P_0,\ldots,P_9$), we obtain up to $N = 97$ different $\mathbf{f}_i$ (the combinations $P_0(\xi)P_0(\eta), P_0(\xi)P_1(\eta)$, and $P_1(\xi)P_0(\eta)$ provide a null $\mathbf{f}_i$ vector). For any polynomial degree of the Airy stress function, $p \geqslant 1$, we obtain $N = (p+1)^2 - 3$ different statically admissible vector functions $\mathbf{f}_i$. The functions $\mathbf{f}_i$ obtained for an Airy polynomial function of order 1, 2 and 3, for example, are provided in Appendix I.

Remark 4. As the radius R of the domain Ω_R varies, it is necessary to scale the variables ξ and η accordingly, and we use ξ/R and η/R in the fuctional expressions for $\mathbf{f}_i$. Otherwise, the condition number of the matrix $[B_c]$ depends on R.

The statically admissible space created by the aformentioned method does not have to satisfy the compatibility equation. Namely, any $\Phi_i(\xi,\eta)$ is a harmonic function satisfying $\nabla^2\Phi_i(\xi,\eta) = 0$, however, we can further restrict $\Phi_i(\xi,\eta)$ to be a bi-harmonic function, which brings us to the next possible statically admissible space.

2.3.2. The equilibrated/compatible space. Any polynomial of the form

$$\Phi(\xi,\eta) \equiv \sum_{i=0}^{I} d_i \Phi_i(\xi,\eta) = \sum_{l=0}^{L}\sum_{m=0}^{M} b_{lm}\xi^l\eta^m \tag{15}$$

can be chosen as the Airy stress function from which the vectors $\mathbf{f}_i$ can be constructed by (14). However, if we wish that not only the equilibrium equation be satisfied, but also the compatibility equation, it is necessary to enforce that $\nabla^4\Phi_i(\xi,\eta) = 0$. This condition imposes a restriction on the coefficient b_{lm} (and therefore on d_i) in (15) (see Reference 13, pp. 516–518):

$$(l+2)(l+1)l(l-1)b_{l+2,m-2} + 2l(l-1)m(m-1)b_{l,m} + (m+2)(m+1)m(m-1)b_{l-2,m+2} = 0 \tag{16}$$

This relationship among groups of three alternate coefficients restricts the number of independent $\mathbf{f}_i$'s, obtained from $\Phi(\xi,\eta)$ using (14), to $N = 4(p+1) - 1$, where $p+2$ is the degree of the complete polynomial function $\Phi(\xi,\eta)$.

A different approach to obtain the same 'equilibrated/compatible' space is by using the complex functions approach by Muskhelishvili, summarized in pp. 262–267 of Reference 14. Any bi-harmonic Airy stress function over a connected domain can be represented by

$$\Phi(\xi,\eta) = \Re\left[\bar{z}\phi(z) + \chi(z)\right] \tag{17}$$

where $z = \xi + \mathrm{i}\eta$, $\phi(z) = \sum_{j=0}^{J}(A_j + \mathrm{i}B_j)z^j$ and $\chi(z) = \sum_{k=0}^{J+1}(E_j + \mathrm{i}F_j)z^j$, and A_j, B_j, E_j, F_j being real constants. After mathematical manipulations performed by symbolic mathematics, one obtains the statically admissible space $\mathbf{f}_i$ from (17) and (14). The 'equilibrated/compatible' functions $\mathbf{f}_i$ for an Airy polynomial function of order 3, 4 and 5, for example, are provided in Appendix I.

3. NUMERICAL EXPERIMENTS WITH THE *p*-VERSION OF THE FEM

3.1. The model problem

Consider the elastostatic problem of an elliptical plate containing an elliptic hole presented in Figure 2, for which the analytic (exact) solution is provided in Reference 3. The domain of interest is bounded by two ellipses, the outer with major axis $a = 4 + m/4$ and minor axis $b = 4 - m/4$, and the inner with $a = 1 + m/1$ and $b = 1 - m/1$. By varying m from 0 to 0·9, we can obtain

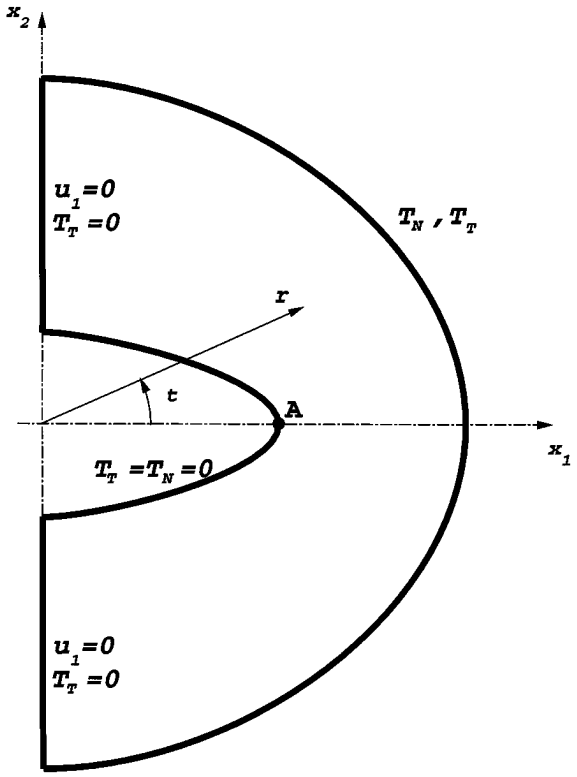

Figure 2. Solution domain and boundary conditions

stress concentration factors at point A (see Figure 2), which range from 3 (corresponding to a circular hole) to 39, respectively. The normal traction component T_{N} and the tangential traction component T_{T} on the outer elliptical boundary are

$$T_{\mathrm{N}}(\theta(t)) = \frac{1}{f^2(4,\theta)}\{\sin 2\theta\,[480(1+m)(16-m^2)+255(m^2+256)] \\ -4080m \sin 4\theta\}$$

$$T_{\mathrm{T}}(\theta(t)) = \frac{1}{f^2(4,\theta)}\{255(256-2m-m^2)(16-m^2)-\cos 2\theta\,[193(256+m^2) \\ +512(m^2+1)]+7200m\cos^2 2\theta\}$$

where $f(4,\theta) = 256 - 32m\cos 2\theta + m^2$ and

$$\theta = \arctan\left\{\left(\frac{16+m}{16-m}\right)\tan(t)\right\}$$

The inner elliptical boundary is stress-free and along the y-axis symmetry boundary conditions are specified, i.e. $u_1 = 0, T_{\mathrm{T}} = 0$. The stresses at any point of the domain are provided in equations (7) and (8) of Reference 3. This model problem, under the assumption of plane stress, Young's modulus 1.0 and Poisson's ratio 0·3, is used in the following to assess the accuracy of the SEC method in conjunction with the p-version of the FEM. Table I summarizes the exact stresses at point A and at point B which is at a distance 0·05 along the x_1-axis for several values of m.

Table I. Exact stresses at points A and B

	$m = 0{\cdot}0$	$m = 0{\cdot}25$	$m = 0{\cdot}5$	$m = 0{\cdot}75$	$m = 0{\cdot}9$
σ_{11} at A	0	0	0	0	0
σ_{22} at A	6·000000000	8·666666667	14·000000000	30·000000000	78·000000000
σ_{12} at A	0	0	0	0	0
σ_{11} at B	0·252981011	0·683559455	1·941701174	5·047253056	6·976223136
σ_{22} at B	5·375136903	6·966601446	8·717152382	9·432508477	9·097850937
σ_{12} at B	0	0	0	0	0

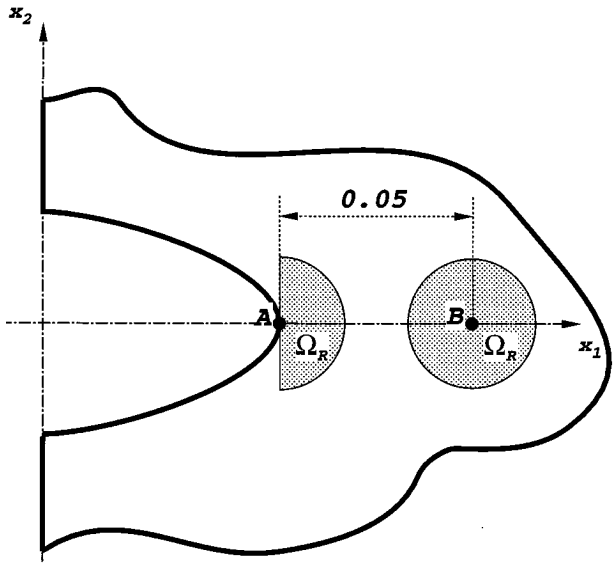

Figure 3. Ω_R domains used for the SEC method

3.2. Numerical results

In the following, we document a convergence study, in which the stresses are extracted from the finite element solution by the SEC and the direct methods as the number of degrees of freedom (DOF) in the finite element model is increased. There are two systematic ways for increasing the number of DOF: the p-version, where the polynomial order over each element is increased while keeping the mesh fixed, and the traditional h-version, where the mesh is successively refined while keeping the polynomial order fixed (usually $p = 1$ or $p = 2$) on each element. Numerical experiments were performed using the computer code STRESS CHECK* which has h- and p-extension capabilities. For solving the model problem by the FEM based on the displacements formulation we used the product space of degree p which spans the set of monomials $\xi^i\eta^j$, $i, j = 0, 1, 2, \ldots, p$, on the standard quadrilateral element defined by $\Omega_{\text{st}}^{(q)} = \{\xi, \eta \,|\, |\xi| \leqslant 1, \ |\eta| \leqslant 1\}$. Elements are mapped by the blending function method, therefore the boundaries are represented exactly in the stiffness matrix and load vector computations. The load vectors were computed by

* STRESS CHECK is Trade Mark of Engineering Software Research and Development, Inc. 7750 Clayton Road, Suite 204, St. Louis, MO 63117, U.S.A.

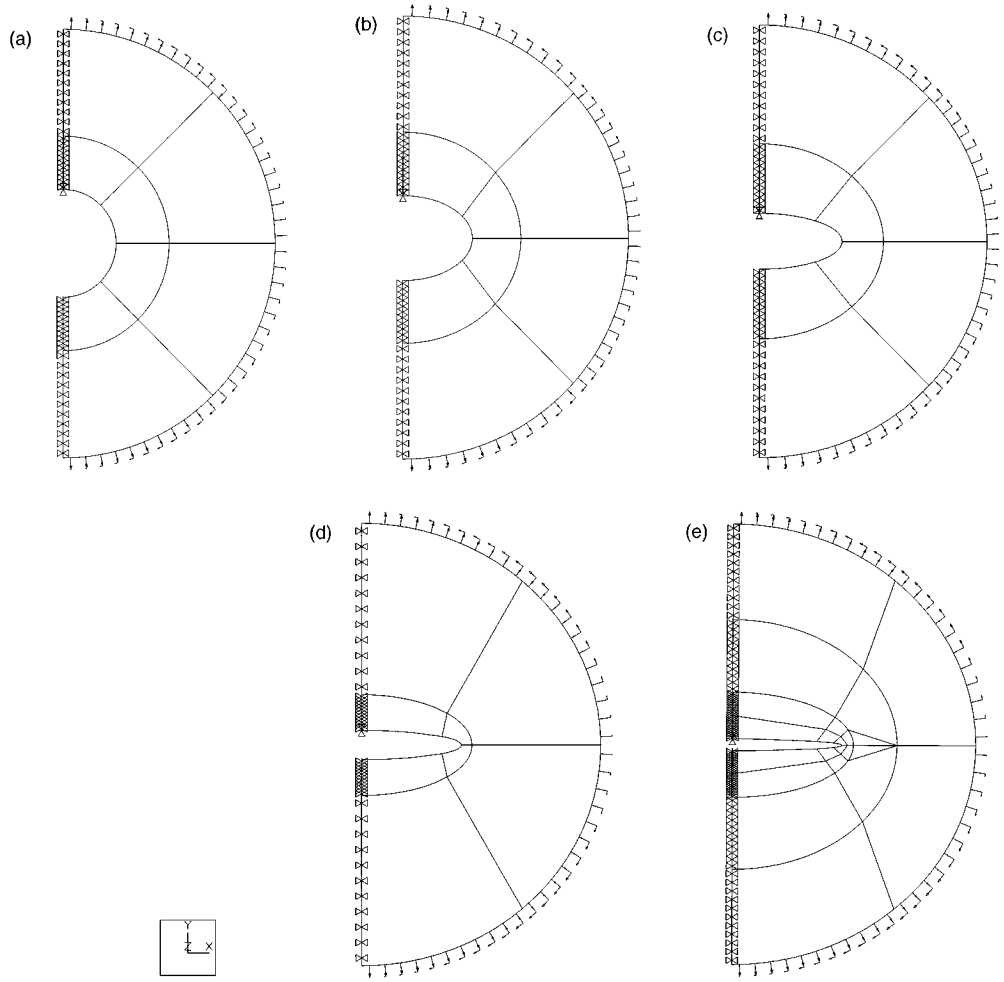

Figure 4. Finite element meshes used in conjunction with the p-version of the FEM: (a) Mesh for $m=0$; (b) Mesh for $m=0{\cdot}25$; (c) Mesh for $m=0{\cdot}5$; (d) Mesh for $m=0{\cdot}75$; (e)Mesh for $m=0{\cdot}9$

evaluating the applied tractions in 14 Gauss points along the loaded edge of each element and integrated numerically, using double precision operations. The trial functions over each element are polynomials of degree $1 \leqslant p \leqslant 8$, and the integration scheme uses $(p+3)(p+3)$ Gauss integration points over each quadrilateral.

In this subsection, the convergence of the extracted stresses from p-version FEM solutions is studied. In order to demonstrate the performance of the SEC method, the stresses are extracted at the boundary point A, where the stress gradient is the highest, and at an interior point B which is $0{\cdot}05$ away from point A along the x-axis. The extraction subdomains Ω_R, used for the SEC method at points A and B are shown in Figure 3. The finite element meshes used in conjunction with the p-version of the FEM for obtaining $\mathbf{u}^{\mathrm{FE}}$ are presented in Figure 4. Numerical experiments performed with both the 'equilibrated' and the 'equilibrated/compatible' statically admissible spaces show that there is a negligible difference in the results when using the same Airy polynomial degree. Nevertheless, the 'equilibrated/compatible' space has a much smaller number of vectors

Table II. SEC stresses at point $(x, y) = (1 \cdot 8, 0)$ for $m = 0 \cdot 75$, $R = 0 \cdot 05$ using the 'equilibrated' and 'equilibrated/compatible' spaces

	σ_{11}		σ_{22}		σ_{12}	
	Equil	Equil/Comp	Equil	Equil/Comp	Equil	Equil/Comp
$p = 1$	3·9115	3·9143	11·4895	11·4935	−2·472E−14	2·378E−14
$p = 2$	3·0818	3·0752	11·4165	11·4080	−1·471E−13	−1·558E−14
$p = 3$	4·1538	4·1529	9·3684	9·3680	3·635E−14	2·266E−14
$p = 4$	4·8587	4·8619	9·2352	9·2415	−7·608E−14	−1·009E−14
$p = 5$	5·0254	5·0319	9·4783	9·4903	3·720E−14	2·533E−14
$p = 6$	5·0004	5·0071	9·4451	9·4581	−1·805E−14	2·263E−14
$p = 7$	5·0200	5·0263	9·3948	9·4073	−3·813E−14	2·686E−14
$p = 8$	5·0422	5·0482	9·4098	9·4218	5·831E−15	2.750E−14
Exact	5·047253		9·432508		0·0	

Condition number of the matrix $[B_c]$ is 1·304944E+13 for the 'equilibrated', and 1·312507E+03 for the 'equilibrated/compatible' space.

$\mathbf{f}_i$ and the associated $[B_c]$ matrix has a considerably smaller condition number as compared with the 'equilibrated' space for the same Airy polynomial degree, therefore the latter has been used in our computation. For example, Table II summarizes the stresses obtained at point $(x, y) = (1{\cdot}8, 0)$ when using the SEC method with an Airy polynomial degree 8, R=0·05, and the finite element solution $\mathbf{u}^{\mathrm{FE}}$ corresponding to p=1–8, for the ellipse characterized by m=0·75.

In the convergence study conducted herein, the three components of the stress tensor, σ_{11}, σ_{22} and σ_{12}, are extracted by the SEC and direct methods, and the relative error in percentage is computed: $100(\sigma^{\mathrm{FE}} - \sigma^{\mathrm{EX}})/\sigma^{\mathrm{EX}}$. Since at point A both $\sigma_{11}^{\mathrm{EX}}$, and $\sigma_{12}^{\mathrm{EX}}$ are identically zero, and at point B $\sigma_{12}^{\mathrm{EX}} = 0$, the relative error of these quantities are not shown. Figures 5 and 6 present the convergence pattern of the pointwise stresses at the boundary of the domain and in the interior extracted by the SEC and direct methods as compared to the convergence in energy norm. The radius of Ω_R is taken to be $R = 0 \cdot 05$ when computing stresses at the interior point for all m's shown in Figures 5 and 6. On the boundaries, for relatively small stress gradients, $m = 0$, 0·25 and 0·5, the radius of Ω_R is chosen to be $R = 0{\cdot}05$. As the stress gradient becomes progressively steep, $m = 0 \cdot 75, 0 \cdot 9$, the integration radius required for high accuracy is reduced for boundary points to $R = 0 \cdot 01$. Figure 5 shows that for boundary points, when the solution is relatively smooth, the convergence rate of the stresses extracted by the SEC method is faster than that of the energy norm, and much faster when compared with the direct method. For interior points, the SEC method is superior to the direct method, and the convergence rate, in general, is similar to that of the energy norm. Figure 6 demonstrates that for boundary points and interior points, when the stress gradients are steep, the SEC method provides stresses which are considerably more accurate than those extracted by the direct method, and the convergence rate is faster than that of the energy norm (at point B for $m = 0 \cdot 9$, no convergence is visible for directly extracted σ_{11}). Nevertheless, the lack of monotonicity observed in the convergence of the pointwise stresses is somewhat disappointing.

The influence of the radius R on the accuracy of the results at interior points is negligible. As an example, we present in Figure 7 the absolute relative error in σ_{11} and σ_{22} for $m = 0{\cdot}0, 0{\cdot}5$ and 0·9 as a function of R at point B, obtained with $\mathbf{u}^{\mathrm{FE}}$ at $p = 8$. However, on the boundaries, for smooth solutions the larger the radius R, the more accurate are the extracted stresses, whereas for steep stress gradients the effect is reversed as shown in Figure 8.

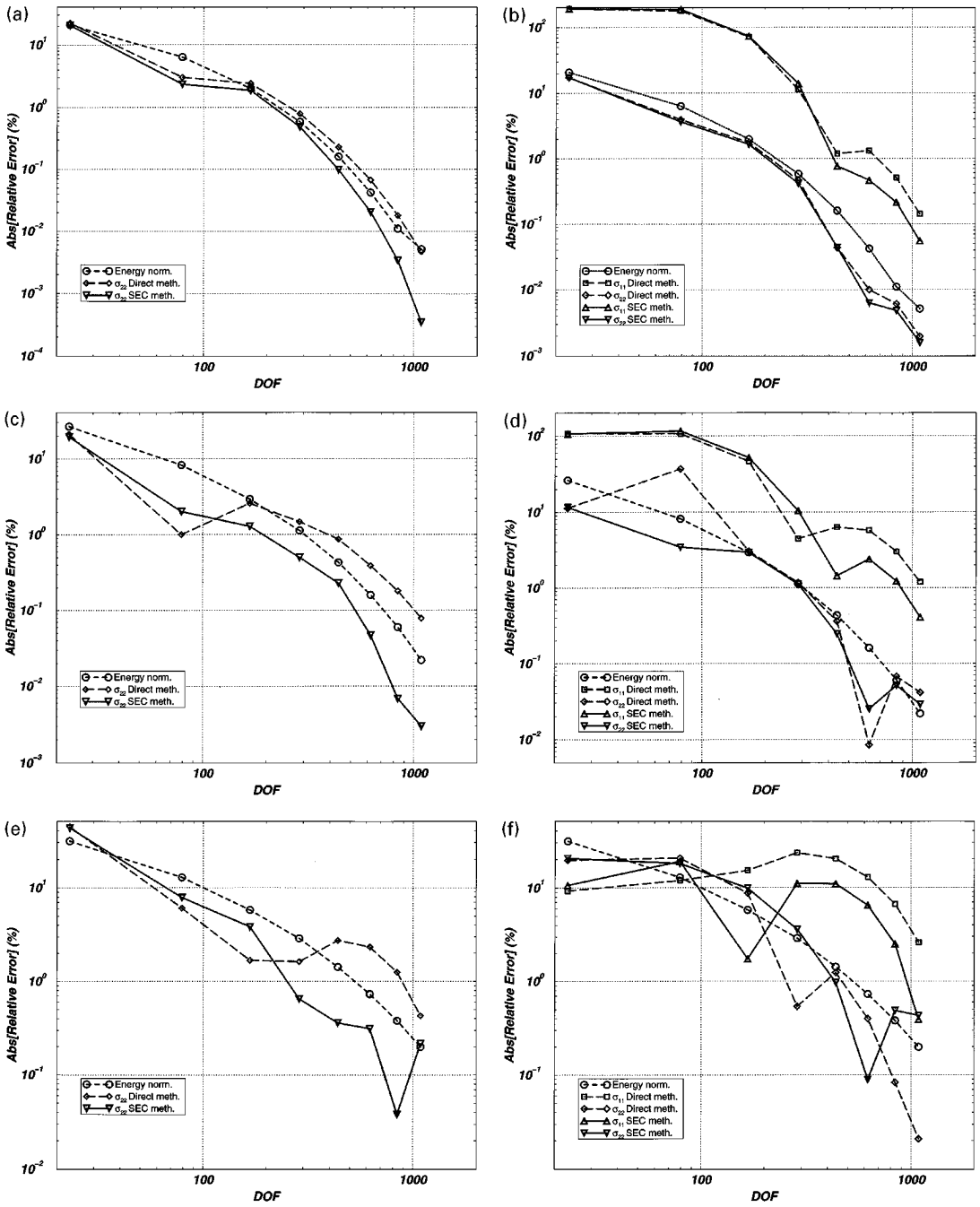

Figure 5. Stress convergence for the p-version of the FEM, $m = 0 - 0{\cdot}5$: (a) Point A, $m = 0$; (b) Point B, $m = 0$; (c) Point A, $m = 0{\cdot}25$; (d) Point B, $m = 0{\cdot}25$; (e) Point A, $m = 0{\cdot}5$; (f) Point B, $m = 0{\cdot}5$

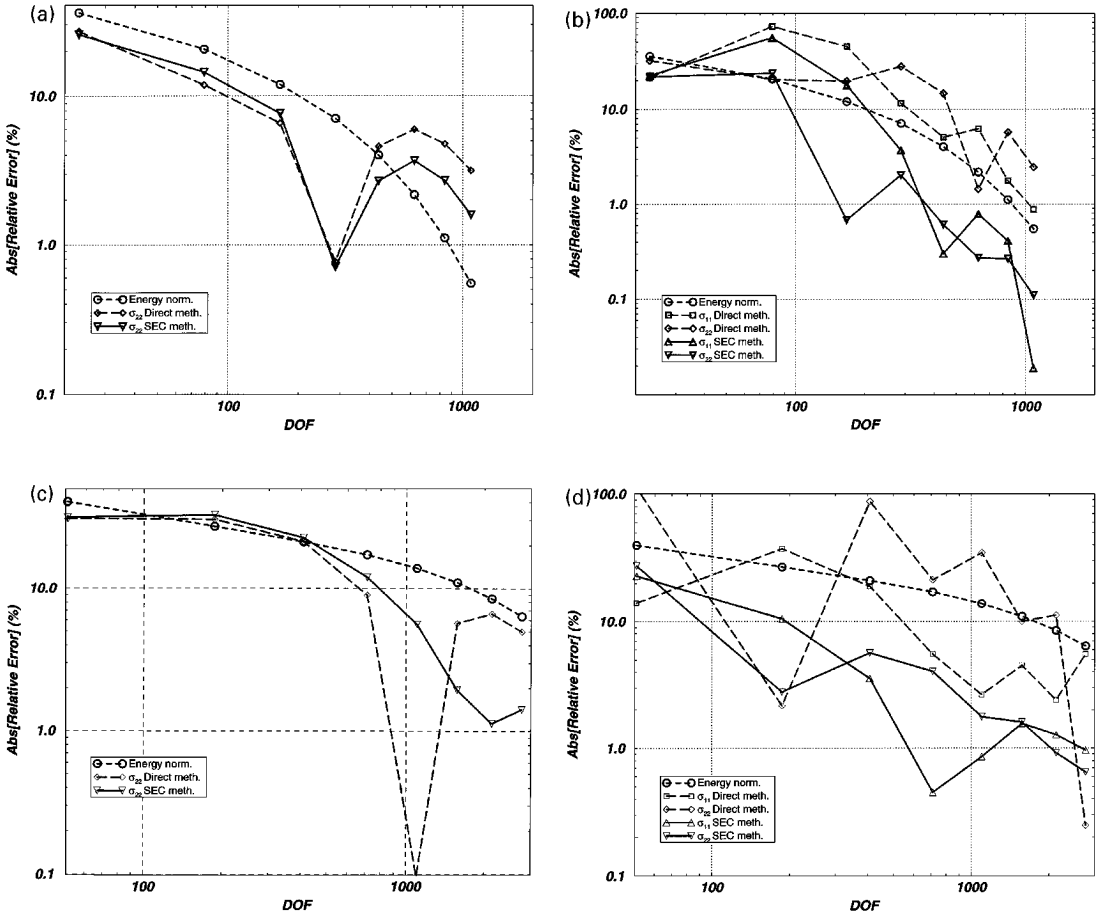

Figure 6. Stress convergence for the p-version of the FEM, $m = 0{\cdot}75 - 0{\cdot}9$: (a) Point A, $m = 0{\cdot}75$; (b) Point B, $m = 0{\cdot}75$; (c) Point A, $m = 0{\cdot}9$; (d) Point B, $m = 0{\cdot}9$

The design of structural components is usually based on yield criterion, such as the von-Mises yield criterion, in which the equivalent stress in 2-D is given by

$$\sigma_{\text{eq}} = \begin{cases} \sqrt{\sigma_{11}^2 + \sigma_{22}^2 - \sigma_{11}\sigma_{22} + 3\sigma_{12}^2}, & \text{plane stress} \\ \sqrt{(1 - \nu + \nu^2)(\sigma_{11}^2 + \sigma_{22}^2) - (1 + 2\nu - 2\nu^2)\sigma_{11}\sigma_{22} + 3\sigma_{12}^2}, & \text{plane strain} \end{cases}$$

Although on the free boundary at point A only σ_{22} is non-zero, the direct method stress extraction will also give a spurious σ_{11} component, which can be quite sizeable, particularly for small number of DOF, and it will give also a spurious σ_{12} component. When commercial FE codes report equivalent stresses, these components are automatically included. Depending on the sign of the spurious σ_{11}, the equivalent stress can be significantly smaller of larger than the exact value. For example, we report in Tables III and IV σ_{11} and σ_{12}, respectively, at point A extracted by the direct and SEC methods for $m = 0$, $0{\cdot}5$ and $0{\cdot}9$.

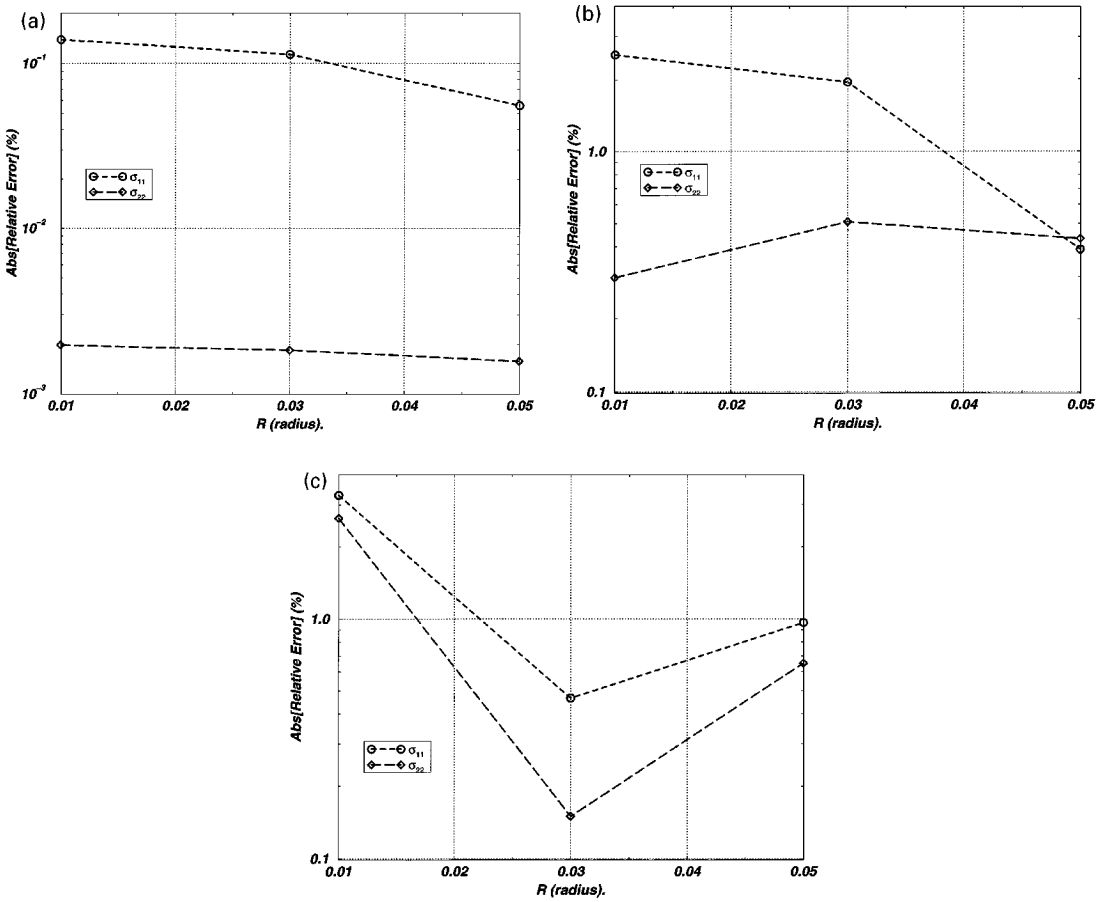

Figure 7. R influence on the stresses at interior point B: (a) $m = 0{\cdot}00$; (b) $m = 0{\cdot}5$; (c) $m = 0{\cdot}9$

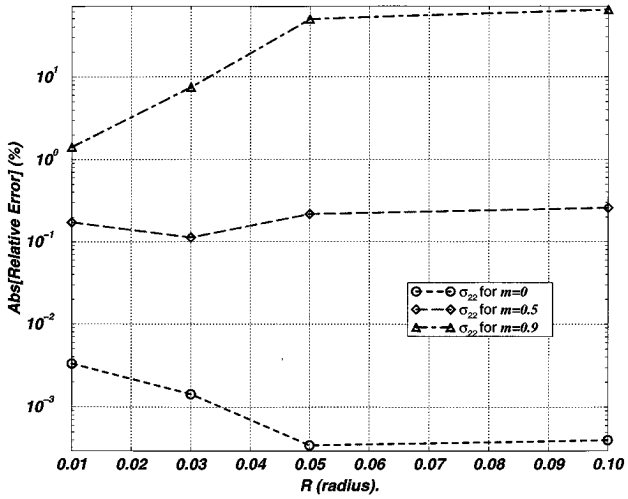

Figure 8. R influence on the stresses at boundary point A

Table III. σ_{11} at point A for $m = 0$, 0·5 and 0·9 extracted by the direct and SEC methods

	$m = 0$		$m = 0{\cdot}5$		$m = 0{\cdot}9$	
	Direct	SEC	Direct	SEC	Direct	SEC
$p = 1$	0·802387	1·301284	2·00972	2·971605	16·4764	12·79713
$p = 2$	0·819469	0·719802	2·82166	2·245907	16·0852	4·700866
$p = 3$	0·446037	0·350214	2·33288	1·460319	16·1784	4·896819
$p = 4$	0·156702	0·091917	1·90849	1·031658	16·3429	2·571864
$p = 5$	0·047647	0·020623	1·42392	0·5049507	16·1835	0·301085
$p = 6$	0·013695	0·004015	0·957308	0·1573321	15·3694	−0·492814
$p = 7$	0·003675	0·000582	0·570323	0·0108936	13·6486	−0·0753866
$p = 8$	0·000932	0·000415	0·307443	−0·029379	11·4608	−0·708049

Table IV. σ_{12} at point A for $m = 0$, 0·5 and 0·9 extracted by the direct and SEC methods

	$m = 0$		$m = 0{\cdot}5$		$m = 0{\cdot}9$	
	Direct	SEC	Direct	SEC	Direct	SEC
$p = 1$	3·21228E−01	5·6319E−11	0·727171	5·4830E−11	1·49784	2·9637E−10
$p = 2$	4·97236E−02	6·5213E−11	0·086842	7·6901E−11	−3·84110	3·0195E−10
$p = 3$	1·22029E−02	6·2844E−11	0·049710	8·0186E−11	−1·26181	4·5912E−10
$p = 4$	−3·02338E−03	6·7381E−11	0·232570	7·8748E−11	0·97339	4·2007E−10
$p = 5$	−2·30773E−04	6·0963E−11	0·199452	7·1040E−11	1·84072	3·3601E−10
$p = 6$	4·43623E−05	5·7203E−11	0·097133	8·7907E−11	1·88657	4·5428E−10
$p = 7$	1·43041E−06	4·6280E−11	0·019792	1·0113E−10	1·66913	4·9389E−10
$p = 8$	−3·21847E−07	7·2205E−11	0·011237	8·0254E−11	1·41999	4·6657E−10

As easily observed in Tables III and IV, the SEC method is much less sensitive to steep stress gradients as compared to the direct method when the spurious stresses are examined.

4. NUMERICAL EXPERIMENTS WITH THE *h*-VERSION OF THE FEM

In this section, the convergence of the extracted stresses from *h*-version FEM solutions is studied. The model problem is the same problem presented in Figure 2. The domain of interest is discretized by laying an *h*-version type mesh with bi-quadratic shape functions ($p = 2$) over each element. Unlike standard FE commercial codes, the boundaries of the elements that lie on the domain boundary are represented accurately, namely they are either ellipses or lines, and not piecewise quadratic. This is achieved by the blending function mapping. A systematic *h*-extension procedure is performed, such that each element is divided into four elements in each refinement cycle. The meshes used in our computation for the case $m = 0$ and $m = 0{\cdot}5$ have the same number of elements, and the four levels of *h*-refinement used for $m = 0{\cdot}5$, for example, are shown in Figure 9. For the case $m = 0{\cdot}9$, a finer set of meshes were used, as shown in Figure 10. As in the previous section, the pointwise stresses on the boundary at point A, and in the interior, at point B, were extracted by the SEC and the direct methods. The relative error (%) in the stresses, and the relative error in energy norm, for $m = 0, 0{\cdot}5$ and $0{\cdot}9$ at points A and B are plotted against the number of DOF on a log–log scale in Figure 11. Figure 11 shows that the stresses extracted by the SEC, in conjunction with the *h*-version of the FEM, converge in general monotonically, especially for boundary points (of course when the energy norm converges as well). For smooth exact solutions, the SEC outperforms the direct method, and its rate of convergence is similar to that of the energy

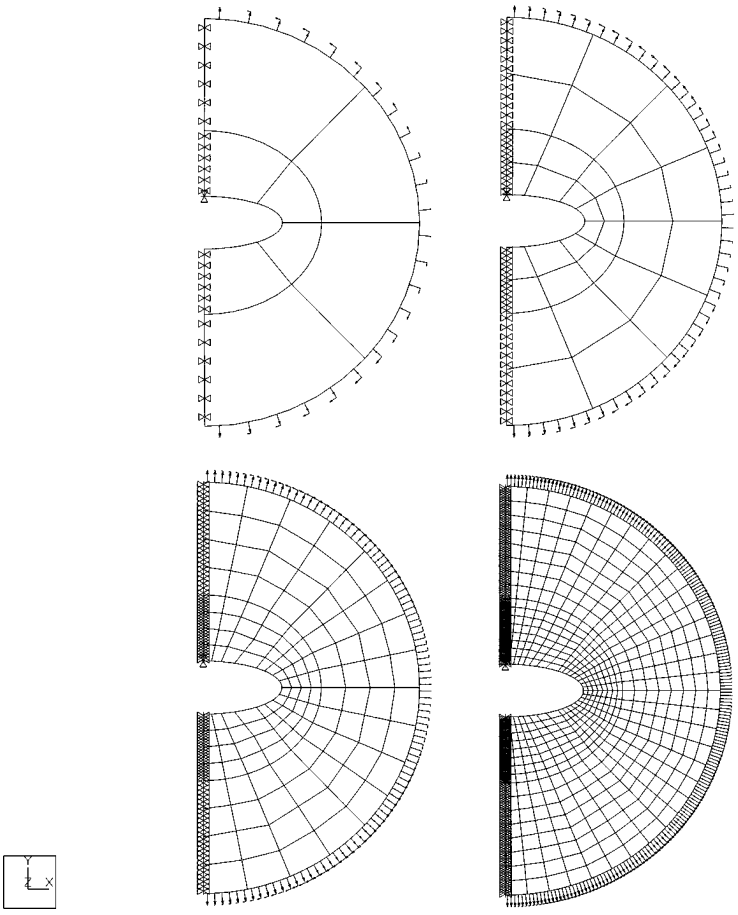

Figure 9. Finite element meshes used in conjunction with the h-version of the FEM, $m = 0{\cdot}5$

norm. As the stress gradient becomes steeper the performance of the SEC deteriorates at boundary points, but improves for interior points (where one of the stress components extracted by the direct method does not converge).

Remark 5. Comparing the convergence rates of the SEC stresses and the energy norm associated with the h-version, to that associated with the p-version of the FEM, one may notice the superiority of the p-version when applied to problems with a regular exact solution. This is especially visible for $m = 0$ and $m = 0{\cdot}5$ (notice that h-extensions are performed with a larger number of degrees of freedom than p-extensions). For $m = 0{\cdot}9$ the pointwise stresses at point A extracted in conjunction with the p-version are more accurate compared to the ones extracted from h-version FEM (this is not so for point B).

5. SUMMARY AND CONCLUSIONS

A new extraction method for computing pointwise stresses from finite element solutions is presented for two-dimensional linear elasticity. The method, denoted by SEC, is based on the principle of complementary energy applied over a circular-type subdomain in the post-processing phase. It

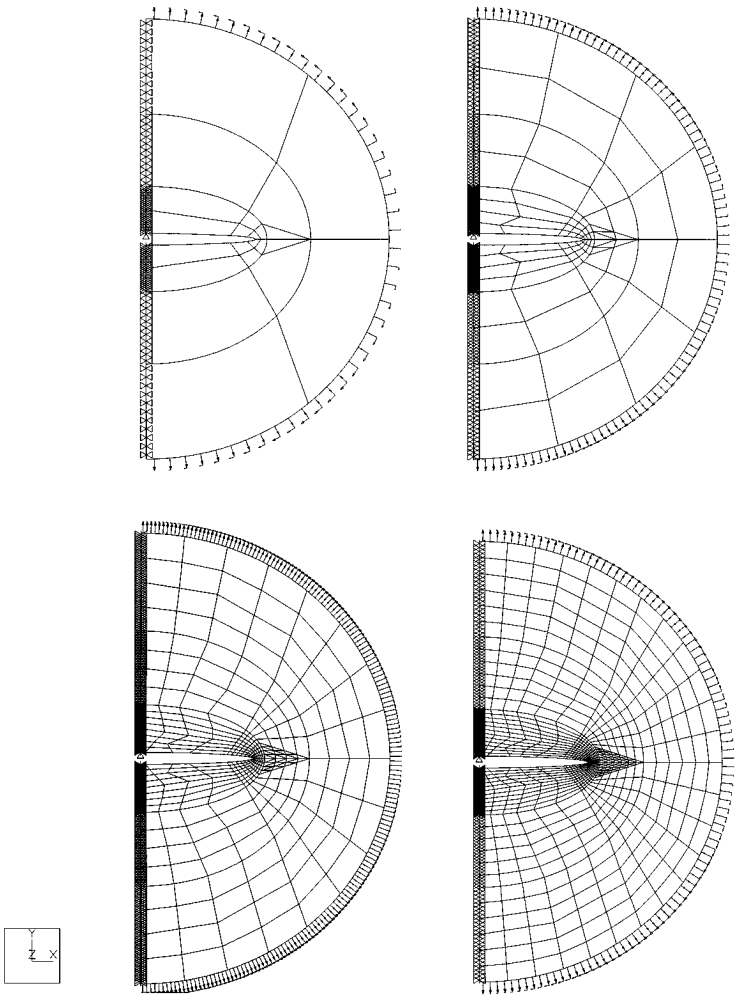

Figure 10. Finite element meshes used in conjunction with the *h*-version of the FEM, $m = 0{\cdot}9$

is applicable to both interior points and boundary points with any specified boundary conditions, as well as to points where the exact solution is singular,[11, 12] and to nearly incompressible materials.[1] Once the location of high stress gradients is determined by standard direct methods, the SEC method could be employed to extract accurately pointwise stresses and to serve as a quantitative measure for the necessity of adaptive procedures.

The numerical performance of the SEC method has been documented based on a set of benchmark problems (for which the exact solutions are known), characterized by a varying degree of smoothness. Numerical results indicate that the gain in accuracy through the SEC method is significant and cost effective. The SEC method is also efficient in terms of CPU time, which requires about 3–4 s on an Indigo2 200 MHz SGI for obtaining the three stress components extracted from eight FE solutions. When stress components are zero at boundaries, or at symmetry/antisymmetry points, they are correctly computed by the SEC method unlike direct methods which usually report spurious stresses.

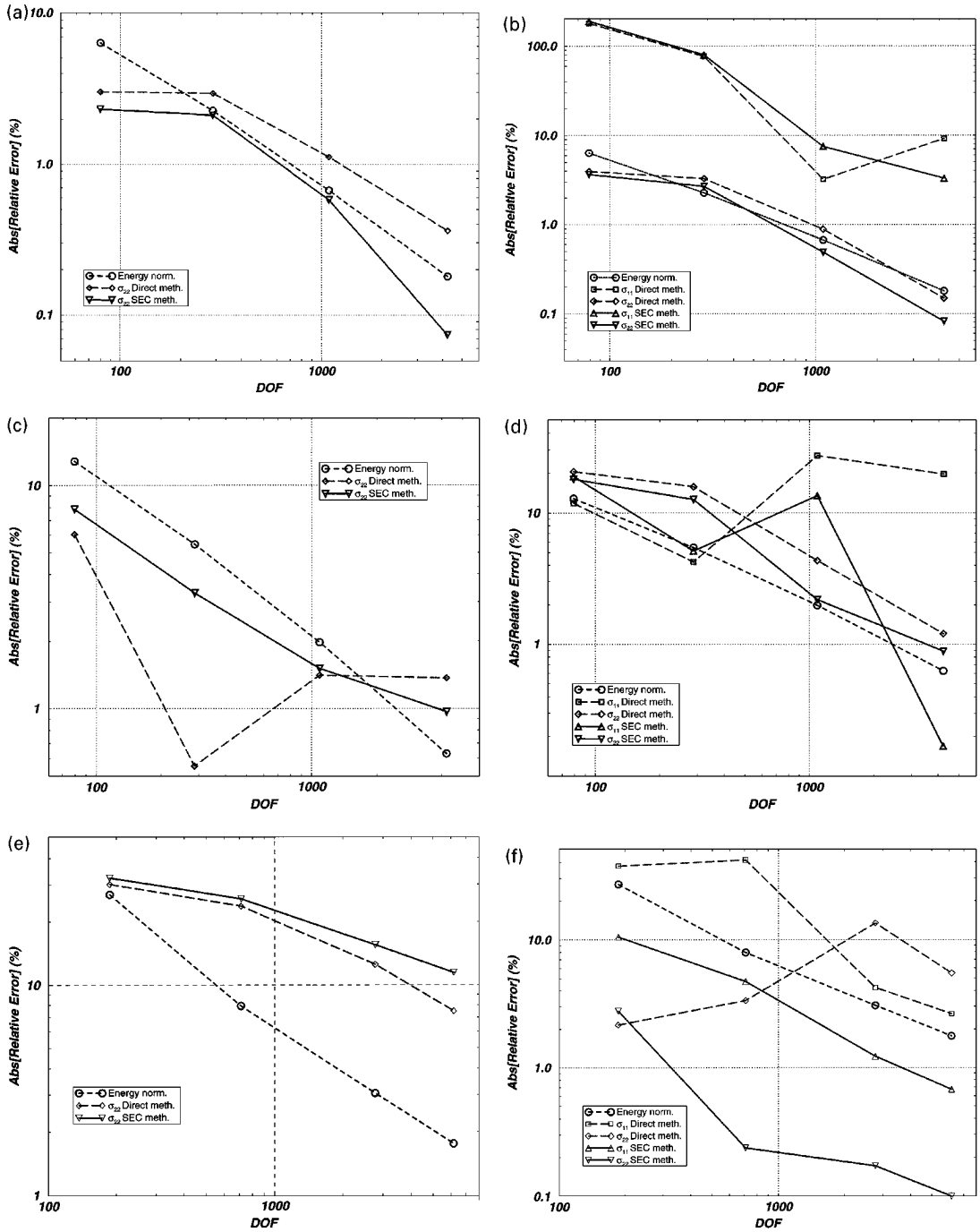

Figure 11. Stress convergence for the *h*-version of the FEM: (a) Point A, $m = 0$; (b) Point B, $m = 0$; (c) Point A, $m = 0{\cdot}5$; (d) Point B, $m = 0{\cdot}5$; (e) Point A, $m = 0{\cdot}9$; (f) Point B, $m = 0{\cdot}9$

It is shown that the relative error in the stresses extracted from finite element solutions based on the *p*-version of the FEM converge in general as fast as the relative error in energy norm or faster (although not monotonically). Numerical experiments indicate that the radius of the circular-type subdomain employed for the extraction should be small for steep stress gradients and large for smooth solutions. Stresses extracted by the SEC method from *h*-version FE solutions converge as fast as the energy norm, or faster, at interior points for all the stress gradients tested. At boundary points, however, the accuracy deteriorates as the stress gradients become steeper.

From the user's point of view the SEC method is simple to use and is general. One has to specify only two parameters: the point of interest within the domain and the radius of integration (the value of N is to be determined adaptively such that the results become virtually unchanged as N is increased). If the point of interest is on the boundary or in its neighbourhood, the SEC is applied automatically on half of a circle, otherwise the subdomain of integration is the whole circle. This method can be used easily with any finite element analysis program.

Based on the documented results, further investigation is under consideration: The application of the SEC method goes beyond pointwise stress extraction, and attention will be focused on error estimation in adaptive analysis by examining the difference in stresses computed by the direct and the SEC methods. At boundary points, a restriction can be imposed on the system of equations, restricting degrees of freedom corresponding to stress components which are known (boundary conditions), therefore improving the accuracy of the extracted stresses.

ACKNOWLEDGEMENTS

The author thanks Prof. Barna A. Szabó for his support and interest in this work, including many helpful remarks and invaluable suggestions. Special thanks are extended to Profs. Ivo Babuška, Manil Suri and Soren Jensen for helpful suggestions and remarks received during the investigation. The equilibrated stress field based on Legendre polynomials was derived and provided to the author by Prof. Szabó and Mrs. Liliana Ventura-Actis, for which many thanks.

APPENDIX I

The statically admissible space

Herein we provide an example of the statically admissible shape functions for the 'equilibrated' and the 'equilibrated/compatible' spaces.

Table V. The equilibrated statically admissible space

i	$(f_{11})_i$	$(f_{22})_i$	$(f_{12})_i$
1	0	0	1
2	0	1	0
3	0	η	$-\xi$
4	$3\xi^2$	$3\eta^2$	$-6\xi\eta$
5	ξ	0	$-\eta$
6	1	0	0
7	0	ξ	0
8	0	$10\xi\eta$	$-5\xi^2$
9	$\xi(5\xi^2-3)$	$\xi(15\eta^2-5)$	$\eta(3-15\xi^2)$
10	$\xi\eta(10\xi^2-6)$	$\xi\eta(10\eta^2-6)$	$-(15\xi^2\eta^2-3\xi^2-3\eta^2)$
11	$\eta(15\xi^2-5)$	$\eta(5\eta^2-3)$	$\xi(3-15\eta^2)$
12	$10\xi\eta$	0	$-5\eta^2$
13	η	0	0

Table VI. The equilibrated/compatible statically admissible space

i	$(f_{11})_i$	$(f_{22})_i$	$(f_{12})_i$
1	1	1	0
2	-1	1	0
3	0	0	1
4	ξ	3ξ	$-\eta$
5	-3η	$-\eta$	ξ
6	-3ξ	3ξ	3η
7	3η	3η	3ξ
8	$-6\eta^2$	$6\xi^2$	0
9	$-6\xi\eta$	$-6\xi\eta$	$3(\xi^2+\eta^2)$
10	$6(\eta^2-\xi^2)$	$-6(\eta^2-\xi^2)$	$12\xi\eta$
11	$12\xi\eta$	$-12\xi\eta$	$6(\xi^2-\eta^2)$
12	$-2\xi^3-18\xi\eta^2$	$10\xi^3-6\xi\eta^2$	$6(\xi^2\eta+\eta^3)$
13	$10\eta^3-6\xi^2\eta$	$-2\eta^3-18\xi^2\eta$	$6(\xi\eta^2+\xi^3)$
14	$30\xi\eta^2-10\xi^3$	$-30\xi\eta^2-10\xi^3$	$-10\eta^3+30\xi^2\eta$
15	$-10\eta^3+30\xi^2\eta$	$10\eta^3+30\xi^2\eta$	$10\xi^3-30\xi\eta^2$

REFERENCES

1. Z. Yosibash, 'Accurate stress extraction for nearly incompressible materials by the displacement formulation of the *p*-version FEM', *Commun. numer. methods eng.*, in press
2. B. A. Szabó and I. Babuška, *Finite Element Analysis*, Wiley, New York, 1991.
3. Z. Yosibash and B. A. Szabó, 'Convergence of stress maxima in finite element computations', *Commun. numer. methods eng.*, **10**(9), 683–697 (1994).
4. I. Babuška and A. Miller, 'The post-processing approach in the finite element method—Part 1: calculation of displacements, stresses and other higher derivatives of the displacements', *Int. j. numer. methods eng.*, **20**, 1085–1111 (1984).
5. I. Babuška, K. Izadpanah and B. A. Szabó, 'The postprocessing technique in the finite element method. The theory and experience', in H. Kardestuncer (ed.), *Unification of Finite Element Methods*, Elsevier, North-Holland, 1984, pp. 97–121.
6. D. Vasilopoulos, 'Extraction of two-dimensional stresses on the boundary', *GMR Research Publication GMR-7459*, 23 August 1991.
7. Q. Niu and M. K. Shephard, 'Superconvergent extraction techniques for finite element analysis', *Int. j. numer. methods eng.*, **36,** 811–836 (1993).
8. O. C. Zienkiewicz and J. Z. Zhu, 'Superconvergence patch recovery and a posteriori error estimates. Part 1: the recovery technique', *Int. j. numer. methods eng.*, **33,** 1331–1364 (1992).
9. M. Tabbara, T. Blacker and T. Belytschko, 'Finite element derivative recovery by moving least square interpolants', *Comput. methods appl. mech. eng.*, **117,** 211–223 (1994).
10. C. Susanne Brenner and L. Ridgway Scott, *The Mathematical Theory of Finite Element Methods*, Springer, Berlin, Heidelberg, New York, 1994.
11. Z. Yosibash and B. A. Szabó, 'Numerical analysis of singularities in two-dimensions. Part 1: computation of eigenpairs', *Int. j. numer. methods eng.*, **38**(12), 2055–2082 (1995).
12. B. A. Szabó and Z. Yosibash, 'Numerical analysis of singularities in two-dimensions. Part 2: computation of the generalized flux/stress intensity factors', *Int. j. numer. methods eng.*, **39**(3), 409–434 (1996).
13. L. E. Malvern, *Introduction to the Mechanics of a Continuous Medium*, Prentice-Hall, Englewood Cliffs, N.J., 1969.
14. I. S. Sokolnikoff, *Mathematical Theory of Elasticity*, McGraw-Hill, New York, 1956.